International Journal of Basic and Applied Sciences, 14 (8) (2025) 608-615

International Journal of Basic and Applied Sciences

Website: www.sciencepubco.com/index.php/IJBAS
https://doi.org/10.14419/896a5439
Research paper

Effect of Nanocellulose Reinforcement on The Structural, Dielectric, and Electrical Breakdown of Epoxy Nanocomposites

M. Michael [1], M. Z. H. Makmud [1] *, Z. Jamain [1], K. N. M. Amin [2], H. A. Illias [3], S. Z. Dabbak [4]

[1] Energy Lab, Green Technologies and Advanced Matter (GREAT) Research Group, Faculty of Science and Technology, Universiti Malaysia Sabah, 88400 Kota Kinabalu, Sabah, Malaysia
[2] Faculty of Chemical and Process Engineering Technology, College Engineering Technology, Universiti Malaysia Pahang Al-Sultan Abdullah, Gambang, Kuantan, Pahang, Malaysia
[3] UM High Voltage Laboratory (UMHVL)، Department of Electrical Engineering, Faculty of Engineering, University of Malaya, Kuala Lumpur, Malaysia
[4] Electrical Engineering Department, Faculty of Engineering and Technology, Al Zaytona University of Science and Technology-zust, Salfit, Palestine
**Corresponding author E-mail: mzhilmey@ums.edu.my*

Received: December 6, 2025, Accepted: December 24, 2025, Published: December 31, 2025

Abstract

This study investigates the influence of nanocellulose (NC) on the dielectric and electric field properties of epoxy-based nanocomposites for high-voltage insulation applications. Two types of NC, cellulose nanocrystals (CNC) and cellulose nanofibers (CNF), were incorporated into an epoxy matrix at loadings of 0.5–5.0 wt.%. Morphological analysis by scanning electron microscopy revealed uniform dispersion at low concentrations and increasing agglomeration at higher loadings, particularly in CNF due to its fibrous structure. Electrochemical impedance spectroscopy showed that composites containing 1.0 wt.% CNC and 0.5 wt.% CNF achieved optimal dielectric performance, with reduced relative permittivity ($\varepsilon_r \approx 5.07$ for CNC and 5.57 for CNF), suppressed conductivity, and stable capacitive behaviour. COMSOL simulations supported these findings, demonstrating reduced peak electric field intensity (25.8 MV/m) at optimal loadings, indicating improved field uniformity. Breakdown strength tests further confirmed the trend, with CNC at 1.0 wt.% exhibiting 57.9 kV/mm (39% higher than neat epoxy) and CNF at 0.5 wt.% showing 46.7 kV/mm (12% higher than neat epoxy). At higher loadings, aggregation increased permittivity, field crowding, and dielectric loss, leading to reduced insulation performance. Overall, CNC provided broader reinforcement potential than CNF, highlighting nanocellulose as a promising sustainable filler for high-performance epoxy insulation.

Keywords: *Nanocellulose; Cellulose Nanocrystals (CNC); Cellulose Nanofibers (CNF); Dielectric; Electric Field; High Voltage Insulation.*

1. Introduction

The development of advanced insulating materials is crucial to ensuring the safety, efficiency, and reliability of modern electrical systems. Among these materials, epoxy resin is widely utilized due to its excellent mechanical strength, chemical resistance, and ease of processing (Adnan et al., 2019) However, epoxy resin exhibits performance limitations when subjected to high-voltage electrical stress, particularly in demanding or variable environments.

To overcome these limitations, researchers have explored the incorporation of nanoscale fillers into polymer matrices to create polymer nanocomposites with improved electrical properties. One of the most promising bio-based fillers is nanocellulose (NC). There are few types of NC such as cellulose nanocrystals (CNC) and cellulose nanofibers (CNF). The raw nanocellulose material from plants cells wall was treated with mechanical treatment to get CNF and further purification by using chemical treatment will create CNC. CNC usually has a rod-like structure whereas CNF has network fiber structure (Amirah Badi et al., 2024; Rostamabadi et al., 2024) These materials possess a high surface area, polar functional groups, and excellent mechanical strength features that contribute to enhanced interfacial polarization and dielectric behavior. NC is also biocompatible and flexible for surface modification. NC has been widely studied in fields such as paper making, packaging, and electronics, its application is now expanding into the high-voltage insulation area. This shift is driven by increasing evidence that natural cellulose-based fillers can enhance dielectric properties. For instance, rice husk, a coarse, bio-based material was shown to improve the structural and dielectric properties of palm oil used in insulation systems (Junian, Makmud, et al., 2021; Junian, Zul Hilmey Makmud, et al., 2021) Similarly, pineapple leaf fiber (PALF) has demonstrated a significant increase in the breakdown strength of polymeric materials (Salleh et al., 2020) These materials are less refined than CNC or CNF because there is lignin on it which can be treated chemically, yet they already yield measurable improvements (El Achaby et al., 2018) In addition, CNC also shows significant

improvement in discharge withstandability and dielectric loss showing a promising result for further development (Makmud et al., 2024). Given that CNC and CNF are nanosized and more structurally uniform, they are expected to produce an even greater enhancement in dielectric performance.

Moreover, nanocellulose is a renewable and environmentally friendly alternative to conventional fillers, aligning with the shift toward green and sustainable material technologies in power systems. Despite increasing interest, the exact influence of epoxy/NC nanocomposite on the dielectric breakdown and electric field behavior of epoxy-based nanocomposites remains underexplored. A limited number of studies have employed a combined experimental and computational approach to investigate how these nanostructures interact with epoxy matrices across different scales. A review of the existing literature reveals that most studies primarily emphasize static dielectric measurements, while comparatively limited attention has been given to electric field simulations or the use of interfacial modeling approaches, such as equivalent circuit fitting based on EIS data. Therefore, this study aims to investigate the influence of NC on the dielectric properties and electric field behavior of epoxy nanocomposites. The research combines microstructural analysis using SEM, electrical characterization through impedance spectroscopy, and electric field modeling via COMSOL Multiphysics simulations. This integrated approach seeks to provide a deeper understanding of how nanocellulose morphology and concentration affect the insulating performance of epoxy systems, with relevance to the development of advanced polymer dielectrics for high-voltage applications.

2. Materials and Methods

2.1. Preparation of epoxy/NC nanocomposites

The epoxy resin types used are diglycidyl ether of bisphenol A (DGEBA), and the curing agent is triethylenetetramine (TETA) with ratio of 3:1 respectively. Initially, the epoxy resin was weighed to get a 1 mm thickness of thin film. Table 1 shows the sample abbreviation of different weight percentages (0.5, 1.0, 3.0, and 5.0) wt.% of CNC and CNF. For instance, the samples are referred to as E for neat epoxy and ECNC0.5 for epoxy filled with 0.5% of nanofiller. Initially, the nanoparticle was weighed and stirred with the epoxy resin for 30 minutes. After that, it was ultrasonicated at 50℃ for 30 minutes. The curing agent was then mixed with the mixture and stirred for another 5 minutes. The mixture was poured into a silicone mold and cured for 48 hours at room temperature. Finally, post-curing was done for 3 hours at 100℃ to complete the sample preparation (Fonseca et al., 2020)

Table 1: Sample Abbreviation and Composition

Samples Abbreviation**	Amount of nanocellulose (wt%)		Average Thickness (mm)	
	CNC	CNF	CNC	CNF
E	-	-	0.70	
ECNC0.5	0.5		0.71	
ECNC1.0	1.0		0.59	
ECNC3.0	3.0		0.70	
ECNC5.0	5.0		0.80	
ECNF0.5		0.5		0.70
ECNF1.0		1.0		0.80
ECNF3.0		3.0		0.77
ECNF5.0		5.0		0.70

**E=Neat epoxy, CNC=Cellulose nanocrystals, CNF=Cellulose nanofibers.

2.2. Morphological analysis

To investigate the dispersion and morphological characteristics of epoxy/NC nanocomposite, Scanning Electron Microscopy (SEM) analysis was conducted on the cross-sectional surfaces of the cured nanocomposite samples. Prior to imaging, the fractured surfaces were sputter-coated with a thin layer of gold to enhance electrical conductivity and prevent charging under the electron beam. SEM imaging was performed using a high-resolution field emission SEM at an accelerating voltage of 10 kV. ImageJ software was used to analyze the average clustering of the nanoparticle.

2.3. Dielectric characterization via impedance spectroscopy

The dielectric behavior of the epoxy/NC nanocomposites was analyzed using a Randles Circuit model with R(RC) configuration as shown in Figure 2, which was selected based on its best agreement with the experimental impedance data and the lowest error, as determined through model fitting in Nova software. This model comprising a series resistor, R1, and a parallel resistor, R2, and a capacitor, C, was employed to computationally reproduce the impedance and phase angle response across the measured frequency range from 1 Hz to 1 MHz. From the fitted parameters, resistance and capacitance values were obtained. The capacitance extracted from the model was then used to calculate the relative permittivity (ε_r) at 50 Hz, selected as the standard frequency for power system applications. In addition, the resistance value from the parallel branch (R2) was used to compute the AC electrical conductivity (σ_{ac}).

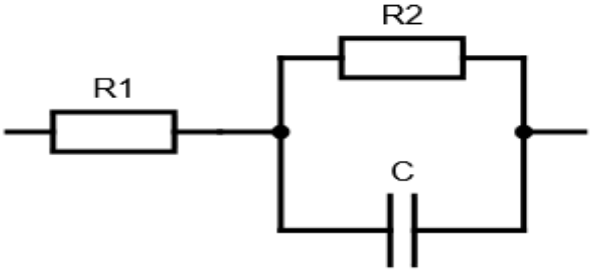

Fig. 2: Randles Circuit Model

2.4. Numerical simulation using COMSOL Multiphysics

The electric field behavior in epoxy/NC nanocomposites, was simulated by using COMSOL Multiphysics. A two-dimensional cross-sectional model of the nanocomposite thin film was developed, as shown in Figure 3, with dimensions corresponding to the experimental setup. The geometry consists of a hemispherical electrode at the top and bottom that is separated by a thin film of epoxy/NC nanocomposite. The surrounding was filled with transformer oil that is similar with physical testing to avoid electrical flashover.
The Electrostatics interface from the AC/DC Module was used in a time-dependent study, enabling simulation of the field distribution under an applied alternating electric field. A sinusoidal voltage of 10 kV peak at 50 Hz was applied to the top electrode, while the bottom electrode was grounded (0 V). All remaining boundaries were treated as electrically insulating to prevent lateral current leakage (Dabbak et al., 2017).
The relative permittivity at 50 Hz and AC conductivity values obtained from equivalent circuit modeling were directly applied to the thin-film domain of each model to accurately reflect the dielectric behavior of the materials. The resulting electric field intensity profiles were exported and analyzed to support the interpretation of experimental dielectric trends and to assess localized field enhancement phenomena associated with filler dispersion and loading.

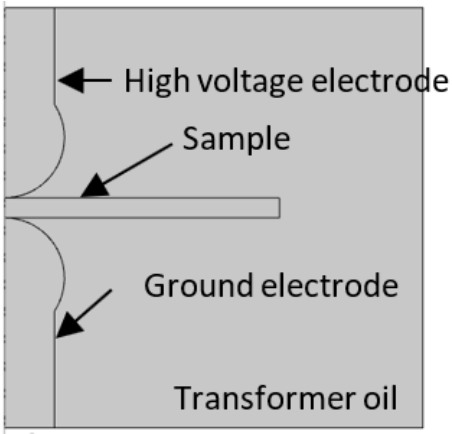

Fig. 3: 2D Model Geometry Used for Electric Field Simulation in COMSOL.

2.5. Electrical breakdown test

The electrical breakdown test was carried out in accordance with the ASTM D149 standard. Figure 4 presents the experimental setup used for the dielectric strength measurement. The test sample was positioned between a pair of spherical stainless-steel electrodes with a diameter of 36.5 mm, as specified by the standard. For the AC breakdown test, an alternating high voltage was applied at a frequency of 50 Hz and increased in a stepwise manner at a rate of 1 kV every 20 s until electrical breakdown occurred. The breakdown voltage was recorded at the point where the sample failed and a conductive path was formed, resulting in circuit closure.

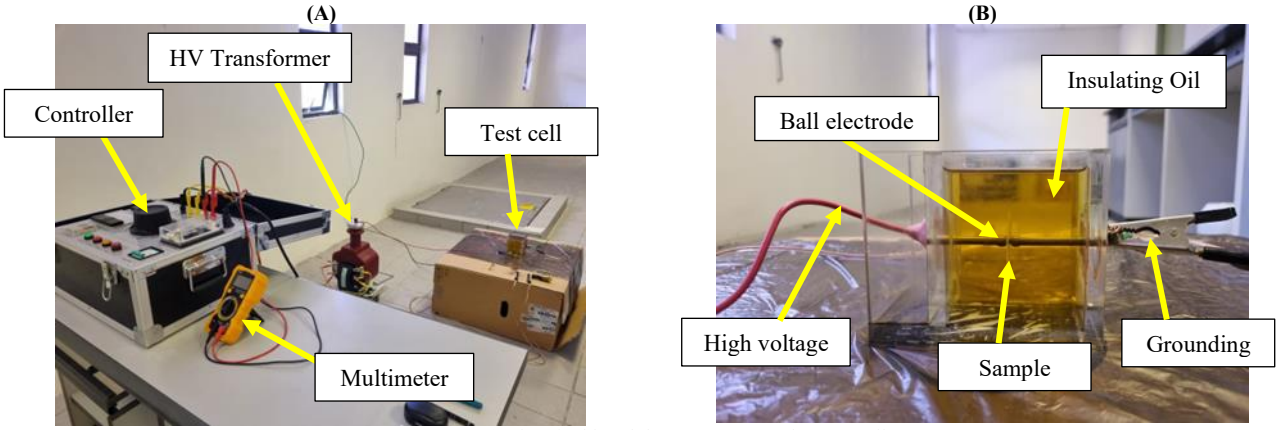

Fig. 4: (a) Electrical breakdown test setup, (b) Test cell.

3. Results and Discussion

3.1. Morphology of epoxy/NC nanocomposites

The microstructural characteristics of the cross-sectional surfaces of the samples were analyzed using SEM, and the corresponding images are shown in Figure 5. The sample containing 0.5 wt.% of CNC and CNF nanofiller in Figure 5(a) and (c) showed that the epoxy matrix was found to have microcrack and less clustering. On Figure 5(b) and (d), a pronounced agglomeration of nanofiller can be observed at higher nanofiller loadings. The presence of CNC may improve microstructural compactness and reduced microporosity (Badi et al., 2024).

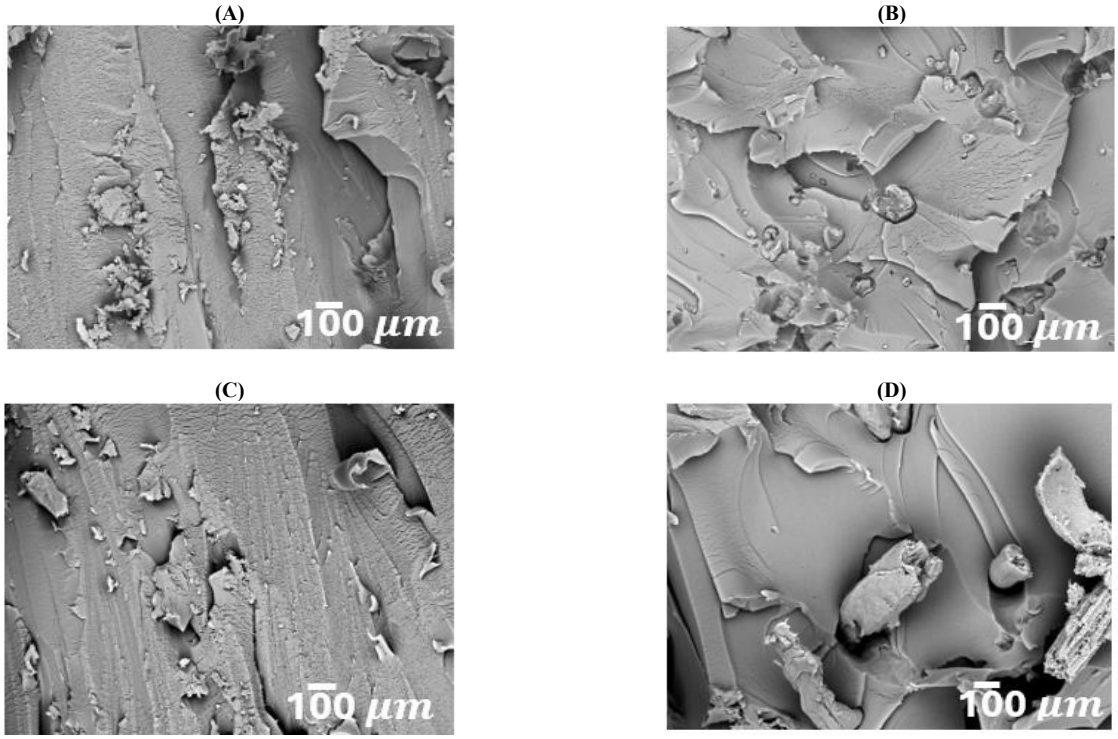

Fig. 5: SEM Micrograph of (a) ECNC0.5, (b) ECNC5.0, (c) ECNF0.5, and (d) ECNF5.0.

Table 2 shows the average clustering diameter of the sample. Sample at higher loadings shows larger clustering size compared to lower loading of nanofiller. The increased agglomeration at higher nanofiller content is likely due to the high surface energy and poor interfacial compatibility at high concentrations, which can hinder effective dispersion and interfacial bonding (Bangar et al., 2022) CNC has high polarity at the surface, which tends to form hydrogen bonding with neighboring particles rather than interacting with the non-polar epoxy in certain regions in the polymer matrix. In contrast, the aggregation on CNF is more pronounced than CNC because of the entangled network structure of CNF (Trache et al., 2020; Xu et al., 2013) Other than that, the epoxy/NC rough structure is similar with previous literature when they prepared bulk mixing via direct mixing without solvent (Qiu et al., 2021)

The addition of NC enhanced microstructural uniformity at lower loadings, but excessive filler content leads to poor dispersion. Severe aggregation could lead to uneven stress transfer to the polymer matrix, which can reduce the mechanical and electrical properties of the polymer nanocomposite (Norrrahim et al., 2021).

Table 2: Average Diameter of Clustering

Sample Code	Average Diameter of Clustering Size, µm
ECNC0.5	46.70±18.31
ECNC5.0	102.88±57.82
ECNF0.5	68.70±19.52
ECNF5.0	215.16±61.07

3.2. Dielectric properties of epoxy/CNC and epoxy/CNF nanocomposites

The impedance and phase angle characteristics of the epoxy/NC nanocomposites were obtained through equivalent circuit modeling based on EIS data. Figure 6 shows the modeled impedance and phase angle responses for the epoxy/NC nanocomposite sample series. As illustrated in Figure 6(a), ECNC1.0 demonstrates the highest impedance across the frequency. ECNC0.5 also shows improved impedance relative to neat epoxy, though slightly lower than ECNC1.0. At higher CNC concentrations (3.0 and 5.0 wt.%), impedance values begin to decline due to poor dispersion at higher loadings leading to greater leakage current, which reduces the impedance value (Román et al., 2018).

All epoxy/CNC nanocomposites exhibit higher phase angles, nearing 90°, compared to neat epoxy, which drops significantly at low frequencies. At mid frequency, all the samples have a consistent value, in high frequency, it drops to 70° which shows that leakage current may be pronounced more at higher frequencies. Nevertheless, the overall nanocomposites retain better capacitive behavior and experience lower dielectric losses at lower frequencies (Cseresnyés et al., 2013).

For the epoxy/CNF series in Figure 6(b), ECNF0.5 shows the highest impedance, whereas ECNF5.0 exhibits the lowest, falling below the impedance of neat epoxy. The trend is the same with CNC where the improvement at low loading is attributed to enhanced filler dispersion, while the performance drop at higher loadings is likely due to CNF entanglement and aggregation, which is more prone to happen on CNF. The corresponding phase angle plot, Figure 6(d) reveals that ECNF0.5 is comparable to neat epoxy, but higher concentrations of CNF result in a marked decrease in phase angle. The phase angle of epoxy/CNF at filler loading (0.5-3.0) wt.% at lower frequency revolves around more than 50°.

In contrast, epoxy/CNC have greater impedance than epoxy/CNF because the nanoparticle dispersion is much better due to the CNC low aspect ratio. Epoxy/CNC able to manage the leakage current well compared to epoxy/CNF (Haeverbeke et al., 2022).

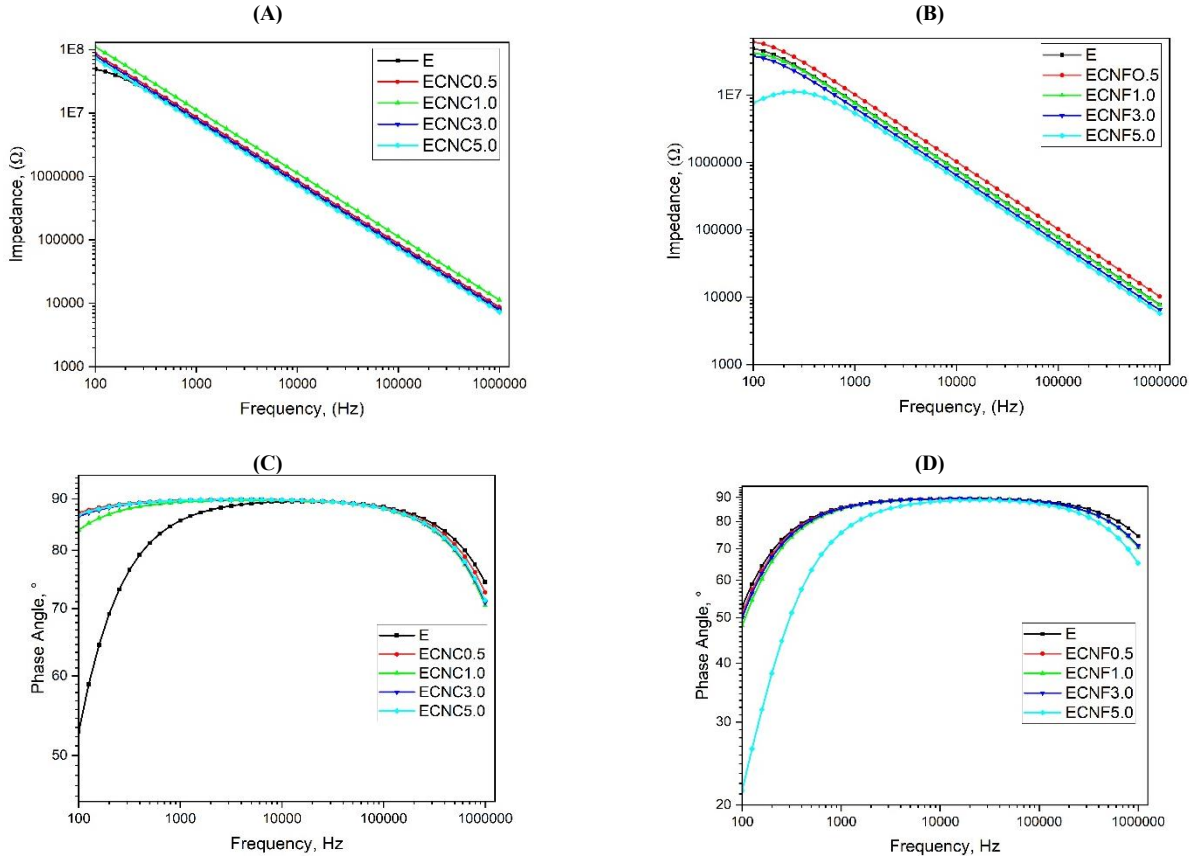

Fig. 6: Impedance and Phase Angle Plots of ECNC and ECNF Nanocomposite: (A) Impedance of ECNC; (B) Impedance of ECNF; (C) Phase Angle of ECNC; (D) Phase Angle of ECNF.

3.3. Computational analysis via equivalent circuit

The dielectric properties of epoxy/CNC nanocomposites are summarized in Table 3. The resistance, R2 of the E was recorded at 0.103 GΩ, and a significant increase was observed in ECNC0.5 reaching 1.780 GΩ. As the filler load increased from 1.0 wt.% to 5.0 wt.%, a drop in resistance was observed with 1.0 wt.% at 1.040 GΩ showing lowest among the epoxy/CNC nanocomposite. The lowest conductivity was observed in ECNC0.5 with 1.79 nSm^{-1}. Epoxy/CNC nanocomposite, with 3.0 wt.% and 5.0 wt.% filler loading, displayed conductivity at 2.47 nSm^{-1}, respectively whereas at 1.0 wt.% filler loading, showed the highest at 3.06 nSm^{-1}. This is due to the formation of a partially connected network of CNCs, where localized clustering or short-range entanglement facilitates limited charge transport through hopping conduction (Kudryashov et al., 2021) Nevertheless, a significant reduction in conductivity was observed when compared to neat epoxies.
Capacitance values show a slight decrease at low CNC loadings (ECNC0.5 and ECNC1.0) compared to neat epoxy, at 18.3 pF and 14.1 pF respectively. As CNC content increases, capacitance rises, reaching 19.8 pF at ECNC3.0 and 21.9 pF at ECNC5.0. A well dispersed CNC in the polymer matrix reduces the dipole movement in the material which is due to more hydrogen bonding with epoxy which causes less polarization, thus the capacitance decreases (El Achaby et al., 2018).
The relative permittivity, ε_r at 50 Hz decreases initially from 7.336 for neat epoxy to 5.071 for ECNC1.0, followed by a marked increase for ECNC3.0 and ECNC5.0, reaching 7.121 and 7.876, respectively. The observed decrease in relative permittivity may be due to the uniform dispersion of CNC in the epoxy matrix, which disrupts the formation of dense hydrogen bonding networks. This increased separation between polar groups reduces dipole alignment and movement under an electric field (Shi et al., 2021).

Table 3: The Dielectric Properties of ECNC

Sample	Resistance, R2 (**GΩ**)	Capacitance, C (pF)	Relative permittivity, $\boldsymbol{\varepsilon_r}$@ 50 Hz	Conductivity, $\boldsymbol{\sigma}$ ($\mathbf{Sm^{-1}}$) x 10^{-9}
E	0.103	20.4	7.336	30.9
ECNC0.5	1.780	18.3	6.581	1.79
ECNC1.0	1.040	14.1	5.071	3.06
ECNC3.0	1.290	19.8	7.121	2.47
ECNC5.0	1.290	21.9	7.876	2.47

Table 4 presents the dielectric properties of nanocomposites with varying CNF loadings. The resistance, R2 of neat epoxy was 0.103 GΩ, while ECNF0.5 showed a slightly lower resistance of 0.127 GΩ, because of the minimal disruption in electrical insulation at low CNF concentration. However, with increasing CNF content, the resistance significantly decreased, reaching 0.225 GΩ at 5.0 wt.%. This reduction implies that higher CNF loadings promote pathways for charge transport or leakage currents (Iyer et al., 2011).
ECNF0.5 with conductivity of 25.1 nSm^{-1} exhibited reduced conductivity compared to neat epoxy. However, the conductivity increased sharply at higher loadings, reaching 141.0 nSm^{-1} for ECNF5.0. This sharp rise indicates the attainment of the percolation threshold at 5.0 wt.% CNF, where a continuous network of interconnected nanofibers facilitates the formation of conductive pathways, thereby enhancing charge carrier mobility throughout the epoxy matrix (Iyer et al., 2011; Saleem & Akbar, 2022) Capacitance values increased progressively with CNF content, from 15.5 pF in ECNF0.5 to 27.8 pF in ECNF5.0. ECNF0.5 has the lowest capacitance compared to the others. At higher filler content, the CNF cluster may accumulate which increase the ability to store energy due to more interfacial polarization occur on the matrix (Wang et al., 2023).

Relative permittivity (ε_r) initially decreased from 7.336 for neat epoxy to 5.574 for ECNF0.5. However, further increases in CNF loading led to a sharp rise in permittivity, with ECNF3.0 and ECNF5.0 reaching 8.847 and 9.998, respectively. The presence of CNF at lower loading can immobilize certain epoxy segments, reduce the mobility of polymer chains and consequently lower electrical polarization mechanisms. This phenomenon leads to a reduction in permittivity, as observed in the nanocomposites, where the interface characteristics significantly influence the overall dielectric properties of the material (Singha & Thomas, 2008).

Table 4: The Dielectric Properties of ECNF

Sample	Resistance, R2 (GΩ)	Capacitance, C (pF)	Relative permittivity, ε_r@ 50 Hz	Conductivity, σ (Sm^{-1}) x 10^{-9}
E	0.1030	20.4	7.336	30.9
ECNF0.5	0.1270	15.5	5.574	25.1
ECNF1.0	0.0850	20.8	7.480	37.4
ECNF3.0	0.0770	24.6	8.847	41.3
ECNF5.0	0.0225	27.8	9.998	141.0

3.4. Electric field intensity

Figure 7 shows the electric field distribution in neat epoxy at a frequency of 50 Hz. The electric field intensity is visualized through a color gradient, where regions of high intensity appear in red and lower intensity in blue. It shows that the electric field intensity of neat epoxy at 40.4 MVm^{-1} is concentrated at the interface between the curved surface of the top electrode and the nanocomposite film. The electric field intensity reduces as it moves away from the electrode tip.

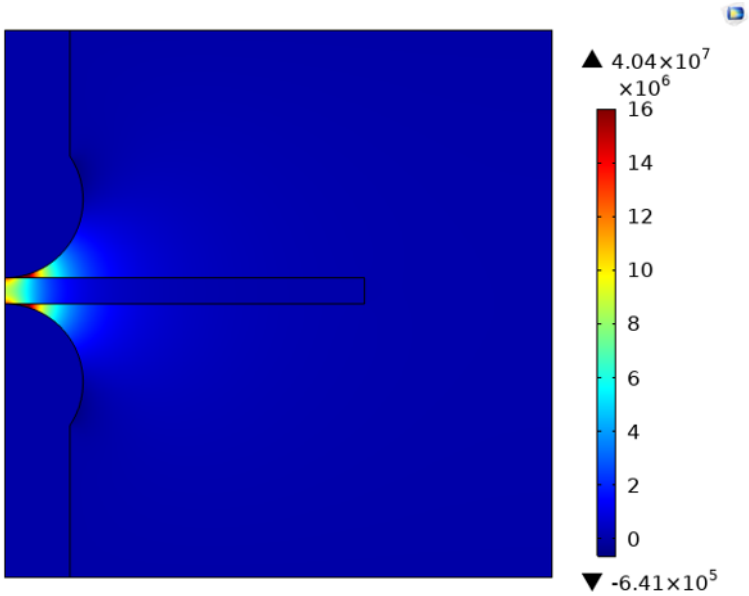

Fig. 7: Simulation of Electric Field Distribution on Neat Epoxy, E, at 50 Hz.

Figure 8 shows the electric field distribution in the epoxy/NC and epoxy/CNF nanocomposites. For the epoxy/NC series, low concentrations (ECNC0.5 and ECNC1.0) result in a reduction of the peak field intensities compared to the neat epoxy. The lowest value for this set is 25.8 MVm^{-1}, recorded at ECNC1.0. However, the field intensity subsequently rises with increasing CNC loading, reaching 38.9 MVm^{-1} in ECNC3.0 and peaking at 44.1 MVm^{-1} for ECNC5.0. In the epoxy/CNF series, the 0.5 wt.% sample (ECNF0.5) also records a low peak field intensity of 28.8 MVm^{-1}. Similar to the CNC samples, increasing the CNF content causes the field intensity to rise again, reaching 51.1 MVm^{-1} for ECNF3.0 and peaking at 59.8 MVm^{-1} for ECNF5.0.

Simulation results revealed that nanocellulose incorporation altered the electric field intensity of epoxy composites. Neat epoxy exhibited a maximum field intensity of 40.4 MVm^{-1} between the electrode and sample interface. At low loadings (0.5–1.0 wt.%), both CNC and CNF reduced the field intensity. This reduction can be attributed to the lower effective permittivity of the composites at low filler loadings, which produced fewer polarization charges at the electrode interface. In addition, the presence of nanocellulose introduced deep traps that immobilized charge carriers and suppressed transport near the electrodes, further reducing local field concentration. As a result, the simulated potential distribution was more uniform, lowering the local electric field. At higher loadings (3.0–5.0 wt.%), however, the effective permittivity and conductivity of the composites increased, which enhanced interfacial polarization and charge transport. This led to stronger field crowding near the electrode tips and raised the maximum field intensity beyond that of neat epoxy. Although the COMSOL model assumes ideal dispersion, the observed trend is consistent with the measured bulk dielectric parameters, which inherently capture the influence of nanofiller dispersion and interfacial effects in real materials.

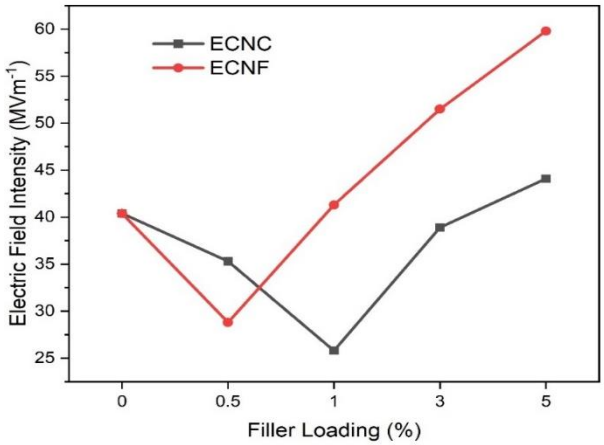

Fig. 8: Electric field intensity comparison for Epoxy/NC Nanocomposite.

3.5. Electrical breakdown strength

The breakdown strength of epoxy and its nanocomposites reinforced with CNC and CNF is summarized in Figure 9. Neat epoxy exhibited a baseline value of 41.6 kV/mm. Incorporation of CNC at 1.0 wt.% produced the highest breakdown strength of 57.9 kV/mm, attributed to efficient dispersion, strong interfacial interaction, and the creation of deep trap sites that suppressed charge transport. A moderate increase was also observed at 0.5 wt.% (47.0 kV/mm), though higher deviation suggested partial agglomeration. Beyond the optimal concentration, breakdown strength declined to 50.2 kV/mm (3.0 wt.%) and further to 40.0 kV/mm (5.0 wt.%), indicating severe filler agglomeration, void formation, and reduced dielectric integrity. Similar trends were reported in PVC/CNC systems (Badi et al., 2024).

For CNF composites, only 0.5 wt.% showed improvement (46.7 kV/mm). At this level, nanofibers likely provided deep traps and tortuous charge paths, delaying dielectric failure. However, increasing CNF to 1.0 wt.% caused a decline below neat epoxy (36.5 kV/mm), reflecting the onset of agglomeration and defect formation. At higher loadings (3.0–5.0 wt.%), breakdown strength deteriorated drastically (16.7–15.7 kV/mm) with large deviations, confirming severe aggregation and poor dispersion that promoted conductive pathways and early breakdown initiation.

Overall, CNC exhibited a broader reinforcement potential than CNF, with an optimal performance at 1.0 wt.%. CNF, despite its higher aspect ratio, was only effective at very low loading. The findings highlight that both nanofillers can enhance dielectric strength but only within narrow concentration ranges. Beyond the threshold, agglomeration and interfacial incompatibility dominate, underlining the need for careful filler optimization and surface modification strategies in high-voltage epoxy insulation.

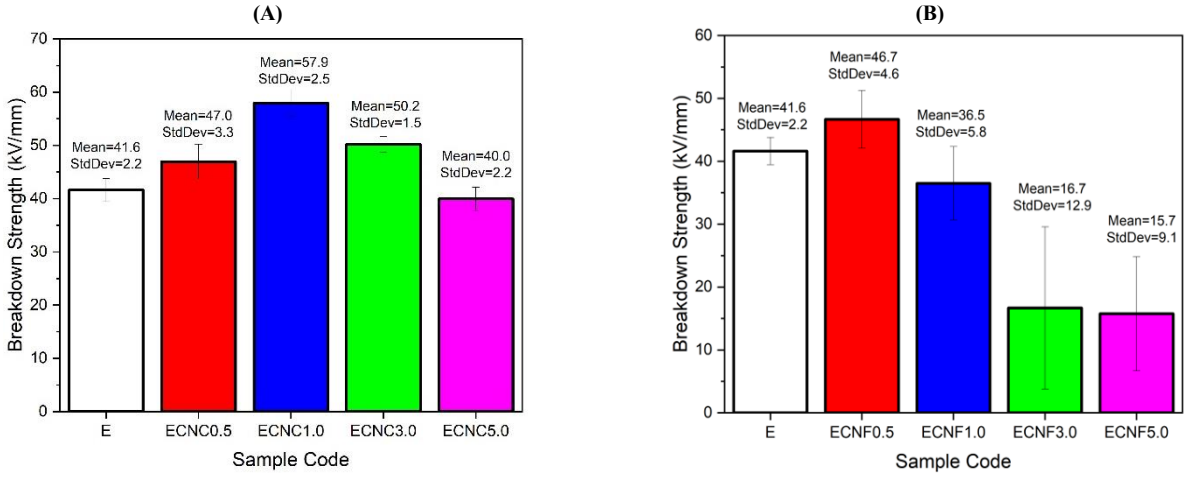

Fig. 9: Dielectric Strength for (a) ECNC and (b) ECNF Nanocomposite.

4. Conclusion

This study showed that the addition of nanocellulose strongly influenced the structure, dielectric properties, and breakdown strength of epoxy nanocomposites. At low loadings, CNC and CNF dispersed more effectively, resulting in lower relative permittivity, improved field uniformity, and stable dielectric response. Simulation results supported these effects by showing reduced electric field intensity near the electrodes. The highest breakdown strength observed in this study was 57.9 kV/mm, achieved by the CNC nanocomposite at 1.0 wt.%. This represents a significant 39% improvement over the neat epoxy. In contrast, the CNF nanocomposite showed only a modest benefit, peaking at 46.7 kV/mm at 0.5 wt.%, which is 12% higher than the neat epoxy. At higher concentrations, the performance of the nanocomposite samples rapidly declined due to nanofiller aggregation, which increased permittivity and reduced insulation performance. The combined experimental and simulation approach provided valuable insights into the structure property performance relationships in nanocellulose-reinforced epoxy nanocomposites, supporting their potential for high-voltage insulation applications.

Funding

This research was funded by the Ministry of Higher Education (MOHE) Malaysia through FRGS Grant Scheme FRGS/1/2023/STG05/UMS/02/2.

Credit author Statement

M. Michael: Investigation, Formal Analysis, Writing – Original Draft, Visualization. M. Z. H. Makmud: Conceptualization, Supervision, Methodology, Writing – Review & Editing, Validation, Project Administration. Z. Jamain & K. N. M. Amin: Supervision, Data Curation & Validation. H. I. Illias & S. Z. Dabbak: Data Curation, Validation.

References

[1] Adnan, M. M., Tveten, E. G., Glaum, J., Ese, M. G., Hvidsten, S., Glomm, W., & Einarsrud, M. (2019). Epoxy-Based Nanocomposites for High-Voltage Insulation: A Review. *Advanced Electronic Materials*, *5*(2). https://doi.org/10.1002/aelm.201800505.

[2] Amirah Badi, N. S., Zul Hilmey Makmud, M., Se Mun, C., Jamain, Z., Asik, J., & Mohd Amin, K. N. (2024). Synthesis and characterization of cellulose nanocrystal derived from paper as nanofiller for polymer insulation materials. *Materials Today: Proceedings*. https://doi.org/10.1016/j.matpr.2023.12.059.

[3] Badi, N. S. A., Makmud, M. Z. H., Jamain, Z., Mohd Amin, K. N., & Illias, H. A. (2024). Enhancement of structural and dielectric properties of PVC/CNC nanocomposites as electrical insulation materials. *Polymers and Polymer Composites*, *32*. https://doi.org/10.1177/09673911241299196.

[4] Bangar, S. P., Harussani, M. M., Ilyas, R. A., Ashogbon, A. O., Singh, A., Trif, M., & Jafari, S. M. (2022). Surface modifications of cellulose nanocrystals: Processes, properties, and applications. In *Food Hydrocolloids* (Vol. 130). Elsevier B.V. https://doi.org/10.1016/j.foodhyd.2022.107689.

[5] Cseresnyés, I., Rajkai, K., & Vozáry, E. (2013). Role of phase angle measurement in electrical impedance spectroscopy. *International Agrophysics*, *27*(4), 377–383. https://doi.org/10.2478/intag-2013-0007.

[6] Dabbak, S. Z., Illias, H. A., & Ang, B. C. (2017). Effect of surface discharges on different polymer dielectric materials under high field stress. *IEEE Transactions on Dielectrics and Electrical Insulation*, *24*(6), 3758–3765. https://doi.org/10.1109/TDEI.2017.006418.

[7] El Achaby, M., El Miri, N., Hannache, H., Gmouh, S., Ben youcef, H., & Aboulkas, A. (2018). Production of cellulose nanocrystals from vine shoots and their use for the development of nanocomposite materials. *International Journal of Biological Macromolecules*, *117*, 592–600. https://doi.org/10.1016/j.ijbiomac.2018.05.201.

[8] Fonseca, E., Demétrio da Silva, V., Klitzke, J. S., Schrekker, H. S., & Amico, S. C. (2020). Imidazolium ionic liquids as fracture toughening agents in DGEBA-TETA epoxy resin. *Polymer Testing*, *87*. https://doi.org/10.1016/j.polymertesting.2020.106556.

[9] Haeverbeke, M. Van, Stock, M., & De Baets, B. (2022). Equivalent Electrical Circuits and Their Use Across Electrochemical Impedance Spectroscopy Application Domains. *IEEE Access*, *10*, 51363–51379. https://doi.org/10.1109/ACCESS.2022.3174067.

[10] Iyer, G., Gorur, R., Richert, R., Krivda, A., & Schmidt, L. (2011). Dielectric properties of epoxy based nanocomposites for high voltage insulation. *IEEE Transactions on Dielectrics and Electrical Insulation*, *18*(3), 659–666. https://doi.org/10.1109/TDEI.2011.5931050.

[11] Junian, S. S., Makmud, M. Z. H., Jamain, Z., Amin, K. N. M., Dayou, J., & Illias, H. A. (2021). Effect of rice husk filler on the structural and dielectric properties of palm oil as an electrical insulation material. *Energies*, *14*(16). https://doi.org/10.3390/en14164921.

[12] Junian, S. S., Zul Hilmey Makmud, M., Dayou, J., & Illias, H. A. (2021). Breakdown Strength and Stability of Palm Oil Toughened with Natural Fibres as Liquid Insulation. *2021 IEEE International Conference on the Properties and Applications of Dielectric Materials (ICPADM)*, *2021-July*, 45–48. https://doi.org/10.1109/ICPADM49635.2021.9493901.

[13] Kudryashov, M. A., Logunov, A. A., Mochalov, L. A., Kudryashova, Y. P., Trubyanov, M. M., Barykin, A. V., & Vorotyntsev, I. V. (2021). Hopping conductivity and dielectric relaxations in ag/pan nanocomposites. *Polymers*, *13*(19). https://doi.org/10.3390/polym13193251.

[14] Makmud, M. Z. H., Michael, M., Rahman, T. A. Z., Jamain, Z., Amin, K. N. M., & Illias, H. A. (2024). Dielectric and Electrical Performance of Epoxy/CNC Nanocomposites for Biomaterial-Based Electrical Insulation. *2024 10th International Conference on Condition Monitoring and Diagnosis (CMD)*, 268–271. https://doi.org/10.23919/CMD62064.2024.10766083.

[15] Norrrahim, M. N. F., Tengku Yasim-Anuar, T. A., Sapuan, S. M., Ilyas, R. A., Hakimi, M. I., Syed Najmuddin, S. U. F., & Jenol, M. A. (2021). Nanocellulose Reinforced Polypropylene and Polyethylene Composite for Packaging Application. In *Bio-based Packaging* (pp. 133–150). Wiley. https://doi.org/10.1002/9781119381228.ch8.

[16] Qiu, K., Tannenbaum, R., & Jacob, K. I. (2021). Effect of processing techniques and residual solvent on the thermal/mechanical properties of epoxy-cellulose nanocrystal nanocomposites. *Polymer Engineering & Science*, *61*(4), 1281–1294. https://doi.org/10.1002/pen.25685.

[17] Román, S., Lund, F., Bustos, J., & Palza, H. (2018). About the relevance of waviness, agglomeration, and strain on the electrical behavior of polymer composites filled with carbon nanotubes evaluated by a Monte-Carlo simulation. *Materials Research Express*, *5*(1). https://doi.org/10.1088/2053-1591/aaa531.

[18] Rostamabadi, H., Bist, Y., Kumar, Y., Yildirim-Yalcin, M., Ceyhan, T., & Falsafi, S. R. (2024). Cellulose nanofibers, nanocrystals, and bacterial nanocellulose: Fabrication, characterization, and their most recent applications. *Future Postharvest and Food*, *1*(1), 5–33. https://doi.org/10.1002/fpf2.12001.

[19] Saleem, M. Z., & Akbar, M. (2022). Review of the Performance of High-Voltage Composite Insulators. *Polymers*, *14*(3). https://doi.org/10.3390/polym14030431.

[20] Salleh, N. I. M., Jamail, N. A. M., Suntharasakan, N., Jamail, N. S. M., Sies, M. F., Kamarudin, Q. E., & Piah, M. A. M. (2020). Analysis of HVDC breakdown characteristic of LLDPE-natural rubber added with biofiller as high voltage insulating material. *Indonesian Journal of Electrical Engineering and Computer Science*, *20*(3), 1203–1209. https://doi.org/10.11591/ijeecs.v20.i3.pp1203-1209.

[21] Shi, S. C., Chen, C., Zhu, J. L., Li, Y., Meng, X., Huang, H. D., & Li, Z. M. (2021). Environmentally friendly regenerated cellulose films with improved dielectric properties via manipulating the hydrogen bonding network. *Applied Physics Letters*, *119*(2). https://doi.org/10.1063/5.0056164.

[22] Singha, S., & Thomas, M. J. (2008). Reduction of Permittivity in Epoxy Nanocomposites at Low Nano-filler Loadings. *2008 Annual Report Conference on Electrical Insulation and Dielectric Phenomena*, 726–729. https://doi.org/10.1109/CEIDP.2008.4772804.

[23] Trache, D., Tarchoun, A. F., Derradji, M., Hamidon, T. S., Masruchin, N., Brosse, N., & Hussin, M. H. (2020). Nanocellulose: From Fundamentals to Advanced Applications. *Frontiers in Chemistry*, *8*. https://doi.org/10.3389/fchem.2020.00392.

[24] Wang, Q., Che, J., Wu, W., Hu, Z., Liu, X., Ren, T., Chen, Y., & Zhang, J. (2023). Contributing Factors of Dielectric Properties for Polymer Matrix Composites. *Polymers*, *15*(3), 590. https://doi.org/10.3390/polym15030590.

[25] Xu, X., Liu, F., Jiang, L., Zhu, J. Y., Haagenson, D., & Wiesenborn, D. P. (2013). Cellulose nanocrystals vs. Cellulose nanofibrils: A comparative study on their microstructures and effects as polymer reinforcing agents. *ACS Applied Materials and Interfaces*, *5*(8), 2999–3009. https://doi.org/10.1021/am302624t.